This article has been accepted for publication in IEEE Transactions on Aerospace and Electronic Systems. This is the author's version which has not been fully edited and content may change prior to final publication. Citation information: DOI 10.1109/TAES.2022.3197098

Deep neural network correlators for GNSS multipath mitigation

Haoqing Li, Parisa Borhani-Darian, Peng Wu, and Pau Closas, *Senior Member, IEEE*

Abstract

Machine learning and, more precisely, data-driven models are providing solutions where physics-based models are intractable. This article discusses the use of deep learning models to characterize the intricate effects of multipath propagation on GNSS correlation outputs. Particularly, we aim at substituting standard correlation schemes, optimal under single-ray Gaussian noise assumptions, with Neural Network (NN)-based correlation schemes, that are able to learn the otherwise challenging to model multipath channels. The paper shows that Deep Neural Networks (DNNs), as applied to tracking loops, can provide enhanced performance as compared to standard correlation schemes in i) Line-of-Sight (LOS) scenarios, by filtering out more noise thanks to strong prior regularization through knowledge of correlation characteristics and Gaussian noise during training process; and ii) at the same time, the DNN can adjust its behavior to better disentangle multipath signals from LOS signals. This article provides results showing the superiority of the proposed DNN trained models, with focus on time-delay tracking in a variety of realistic scenarios.

Index Terms

Deep learning, GNSS, delay-estimation, multipath propagation.

Authors are with the Department of Electrical and Computer Engineering at Northeastern University, 360 Huntington Avenue, Boston, MA 02115 (USA). e-mail: {li.haoq, borhanidarian.p, wu.p, closas}@northeastern.edu

This work has been partially supported by the National Science Foundation under Award ECCS-1845833

Deep neural network correlators for GNSS multipath mitigation

I. Introduction

GNSS has been widely used in position, navigation, and timing applications demanding high accuracy and precision [1]–[4]. The growing dependence on GNSS within critical infrastructures has posed some concerns about the potential threats to Global Navigation Satellite System (GNSS). Therefore, techniques have been studied for years to mitigate the influence of a variety of error sources such as multipath propagation or interference-rich environments [5]–[8]. In GNSS processing, tracking loops are used to continuously estimate the time-evolution of the signal synchronization parameters (namely, code-delay and carrier-phase). In the tracking block, correlation between GNSS signal and local replicas of satellite's pseudo-random codes is a fundamental component that is used to build the so-called Cross Ambiguity Function (CAF), which the receiver aims at optimizing. The described correlation approach used to compute the CAF is $i)$ mathematically simple to implement, but computationally intensive; and $ii)$ optimal under white-Gaussian noise, but easily spoiled in non-nominal situations, such as in the presence of outliers for instance due to multipath conditions. In this paper, we refer to this correlation approach as the *nominal* case or the standard correlation process, given it is the one implemented in all current GNSS receivers. Focusing on distortions due to multipath propagation, as an example, the type of distortions caused in the CAF are such that time-of-arrival estimates become positively biased due to the induced extra propagation path [9]. The physics of this propagation problem are convoluted and depend on many, typically unknown, variables (such as urban/suburban/rural type of scenario, satellite's elevation, or the receiver's speed to name a few). As a consequence, accurate modeling of the propagation channel is a challenging task [10]. This article proposes to leverage data-driven DNN models to learn those multipath models as an alternative to well understood, standard correlation schemes. The main objective being to enable the receiver to maintain tracking accuracy in multipath-rich and noise-dominated environments where traditional correlation-based methods would degrade or even become unreliable.

Many methods have been proposed in the literature in order to mitigate those effects on standard tracking loops, as depicted in Fig. 1. Most of those works are either studying 1) enhanced discriminator

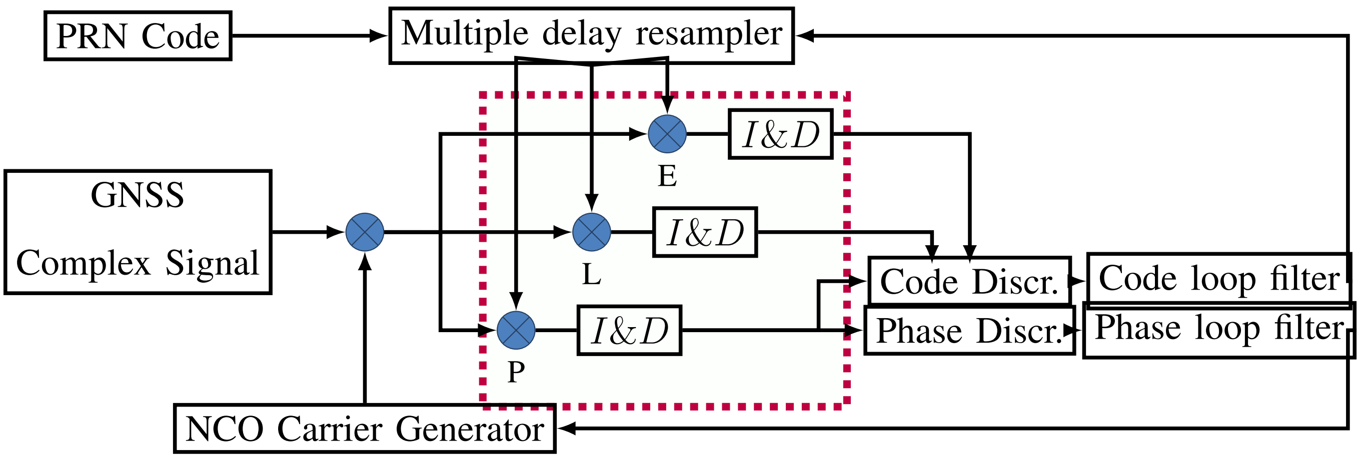

Figure 1: Diagram of a code/carrier tracking loop scheme with standard correlation method using multipliers and Integrate and Dump (I&D) operators.

functions, such that the delay/phase lock loops (DLL/PLL) are less sensitive to multipath effects. For instance, the Narrow Correlator [5], the Pulse Aperture Correlator (PAC) [11], the Double Delta Correlator [6], the Early1/ Early2 (E1/E2) tracking technique [12] or the Multipath Elimination Technology (MET) [13] are classical solutions within that approach; or 2) advanced receiver architectures that jointly estimate the line-of-sight and multipath components for each satellite link, in a typically computationally complex process. For instance, the Multipath Estimating Delay Lock Loop (MEDLL) [7], the Vision Correlator [14], the Multipath Mitigation Technique (MMT) [15], or the use of particle filtering to discriminate among propagation paths [16]. These methods can yield to robust correlation and tracking results, however, it is worth noting that they heavily rely on accurate physics-based models and deviations from those might cause dramatic degradations in performance. In real-world experiments, models might result inaccurate in a variety of situations [17]. This article proposes to substitute correlation-based CAF computations (which inherently rely on physics-based models), with correlation schemes purely derived from a data-driven paradigm in which the complexity of the channel is learned from data.

With the increased popularity of Artificial Intelligence (AI), machine learning and deep learning begin to play an important role in adapting traditional algorithms in a variety of disciplines, especially when it comes to estimation and classification tasks. At a glance, deep learning algorithms (for instance, the variety of NNs architectures currently available) are data-driven models that, instead of using complex-to-derive physics-based models, use vast datasets to learn the correlations in the data. Therefore, a computer uses large datasets to train multiple layers of a NN, in a time-consuming process until acceptable accuracy performance is achieved. When physics-based models are available, as is the case for the so-called correlation used in CAF computation, the use of NNs might seem redundant. However, the appeal of adopting such deep learning methods comes in situations where a physics-based model is either too complex to use or not available at all. This is the case of, for instance, multipath channels as motivated earlier.

Deep learning has been recently used in a variety of GNSS-related topics, with [18] providing an excellent summary. In terms of GNSS for remote sensing and Earth observation, [19] applied a NNs for earthquake detection, [20], [21] proposed Convolution Neural Network (CNN) to track hurricanes and detect sea ice. Furthermore, [22] discussed variations of typical DNNs solving different environmental remote sensing problems. In terms of ionospheric scintillations and tropospheric wet delay, [23], [24] showed Support Vector Machine (SVM) and Decision Tree (DT) to detect scintillation. In [25], Gaussian Process Regression (GPR) was used for the forecasting of low-latitude ionospheric conditions. Estimation of GNSS atmospheric-induced delays has been also attempted using Multilayer Perceptron (MLP) for single frequency receivers [26], CNN [27], and employing an Artificial Neural Network (ANN) for tropospheric wet delay estimation [28]. A survey of ionospheric scintillation monitoring and estimation can be consulted in [29], where the use of machine learning is discussed. Machine learning is becoming increasingly popular in the context of detection and mitigation of jamming, spoofing, and evil waveform threats. For instance, [30]–[34] proposed various NN-based supervised machine learning approaches for spoofing detection (methods including CNN, MLP, RNN based on Long Short-Term Memory (LSTM) and classification SVM (C-SVM) with Principal Component Analysis (PCA)). In [35], the authors proposed SVM and CNN models to detect and classify jamming signals, while a NN was used for evil waveforms detection in [36]. In [37], a MLP is built together with adaptive notch filter for mitigation of narrowband interference. Data-driven models have been successfully used in the context of GNSS/INS integrated systems where, for instance, a Back-Propagation Neural Network (BPNN)-aided integrated navigation method based on vehicle motion learning was proposed in [38] for Strapdown Inertial Navigation System (SINS) position error estimation. More recently, [39] considered a Recursive Neural Network (RNN) based method to estimate errors of the INS and [40] introduced a CNN model within the Kalman filter equations implementing the sensor fusion algorithm.

This article focuses on multipath propagation and the ability of GNSS tracking loops to counteract its effects. In that context, there are several works which are primarily operating at the observable level. Namely, [41]–[47] are a representative set of works which considered various models at the observable-level, including CNN, Adaptive Neuro Fuzzy Inference System (ANFIS) based algorithm, SVM, Robust Gradient-Boosting Decision Tree (GBDT), or LSTM. Similarly, in addition to the GNSS measurements-level processing, deep learning can also improve the performance of signal-level techniques: [48] presented a GNSS signal acquisition method based on various DNN models and [49] applied a DNN to substitute both discriminator and correlator in multipath scenarios. This approach was further extended by integrating the CNN to conduct non-LOS and multipath detection [50]–[53] and mitigation [54].

This article proposes to substitute the correlation operation in GNSS receivers by a data-driven model that learns the complexities of multipath channels, which is particularly suited to overcome the challenges imposed on tracking loops. Correlation of the incoming signal with the satellite's local replica is known to be optimal under the Gaussian assumption for the random noise term. Unfortunately, this assumption does not hold in multipath-rich environments where highly correlated replicas distort the so-called CAF in a way that its optimization does not yield to an unbiased code-delay and carrier-phase estimation. The modeling approach combines a physics-based model (that is, encoding the information that correlation is optimal under nominal conditions) with data-driven modeling to learn the departures from the nominal model under multipath conditions. This article is an extension of [54], where preliminary models and results were discussed. The model substantially changed, making it broadly applicable in both LOS and multipath conditions. While in [54] there was a need to classify LOS/multipath scenarios before computing correlation outputs, this is not anymore needed in the present version of the NN-based correlation model. In the current article, a DNN is used to reconstruct a cleaned version of the CAF. Particularly, a first CNN layer is fed with sample-level I&Q signal which is then followed by an MLP that will produce correlation outputs at arbitrary delay/phase samples as required by the DLL/PLL operation. The input is therefore the complex baseband samples and, accordingly, the output provides both in-phase and quadrature components of the noise-filtered and multipath-mitigated CAF. The model learned the distortions due to the multipath propagation channel through exhaustive training based on single multipath-ray simulation and is tested using the realistic channel model given by the ITU-R Recommendation P.681 [55]. Then, the resulting model was employed in standard DLL/PLL tracking loops and performance tested. It is worth noting that no modifications to DLL/PLL algorithms were required since the proposed model substitutes transparently current correlation blocks. The results show the performance of the proposed NN-based correlation approach considering different kinds of popular discriminators, as well as different propagation scenarios. A standard tracking method using correlation-based CAF-computation was also used for comparison over the same GNSS signal and discriminator, showing that the proposed physics-informed data-driven CAF method outperforms current the legacy solution.

The remainder of the article is organized as follows. We first introduce signal model considered in this paper in Section II. A brief overview of DNN is discussed in Section III, as well as the details of the data-driven model proposed here. Parameters of the proposed NN are discussed in Section IV. Simulation results under different scenarios are analyzed in Section V to show the advantage of the proposed method. Finally, conclusions are provided in Section VI.

II. Signal Model

GNSS signals are spread-spectrum modulated using families of quasi-orthogonal sequences $c_i(\cdot)$ that both uniquely identify the i-th satellite and enables accurate synchronization at the receiver. Since the processing is typically performed on a per-satellite basis, in this article and without loss of generality, we assume a signal model that only considers a single satellite and thus we omit index i when convenient. The signal received by the antenna of a GNSS receiver can be modelled as:

$$y(t) = x(t;\boldsymbol{\theta}) + \sum_{j=1}^{M} x(t;\boldsymbol{\theta}_j) + \eta(t) \tag{1}$$

where

$$x(t;\boldsymbol{\theta}) = \sqrt{2C}d(t-\tau_0)c(t-\tau_0)\cos(2\pi(f_{RF}+f_0)t+\phi_0) \tag{2}$$

is the LOS signal of interest at the receiver. C is the signal power and $d(\cdot)$ is the navigation message. f_0 is the Doppler shift with respect to the nominal signal Radio Frequency (RF), f_{RF}, and τ_0 and ϕ_0 model the delay and phase shift introduced by the communication channel. Notice that $\boldsymbol{\theta} = (\phi_0, \tau_0, f_0)^\top$ is a vector that gathers these parameters, which characterize the useful signal. The second term in (1) denotes the possibly multiple M paths the signal can travel, namely the multipath components. Notice that those signals have the same parametric form as the LOS signal, however with different phase, delay, and Doppler values as denoted by vector $\boldsymbol{\theta}_j$ for the j-th path. Finally, $\eta(t)$ is a zero-mean Additive White Gaussian Noise (AWGN).

After amplification, filtering, down-conversion and sampling at $f_s = \frac{1}{T_s}$, the signal provided by the receiver front-end is a baseband complex sequence:

$$y[n] = x[n;\boldsymbol{\theta}] + \sum_{j=1}^{M} x[n;\boldsymbol{\theta}_j] + \eta[n] \tag{3}$$

$$x[n;\boldsymbol{\theta}] = \sqrt{2C}d(nT_s-\tau_0)c(nT_s-\tau_0)e^{j(2\pi f_0 nT_s+\phi_0)} \tag{4}$$

where n is the time index, and square brackets are used to denote discrete time sequences. $\eta[n]$ is circularly symmetric AWGN with independent and identically distributed (i.i.d.) real and imaginary parts, each with variance σ^2, which together makes the total variance of the complex process $\eta[n]$ equal to $2\sigma^2$. Commonly, σ^2 can be modeled as:

$$\sigma^2 = N_0 B_{Rx} \tag{5}$$

where B_{Rx} is the front-end one-sided bandwidth, and N_0 is the Power Spectral Density (PSD) of $\eta(t)$, the noise in (1).

Generally speaking, the task of the receiver is to estimate the parameters in $\boldsymbol{\theta}$. Particularly, acquisition seeks coarse estimates of τ_0 and f_0, while tracking outcome is a more accurate estimate of those parameters, ϕ_0 and the signal power. This is typically accomplished through ML estimation (MLE), where it is typically assumed that the parameters in $\boldsymbol{\theta}$ are piece-wise constant within the N samples of $\mathbf{y} = (y[0], \ldots, y[N-1])^\top$ and that the codes have ideal cross-correlation properties so they can be processed independently at the receiver. It is known that the solution to such estimation process results in the maximization of the correlation between the received signal and a locally generated code. This correlation operation is encoded in the so-called Cross Ambiguity Function (CAF), which is nothing but the correlation between $y[n]$ and the spreading code of the i-th satellite, at a given delay/Doppler pair (in discrete-time):

$$\mathcal{C}_i(\tau_0, f_0) = \frac{1}{N} \sum_{n=0}^{N-1} y[n] \underbrace{c_i(nT_s - \tau_0) e^{-j2\pi f_0 n T_s}}_{\text{Local replica}} , \tag{6}$$

which can be expressed more compactly in vector notation after gathering N samples from the samples and the local code as $\mathbf{y}, \mathbf{c}_i \in \mathbb{C}^{N\times 1}$ as

$$\mathcal{C}_i(\tau_0, f_0) = \frac{\mathbf{c}_i^H \mathbf{y}}{N} , \tag{7}$$

such that $\mathcal{C}_i(\tau_0, f_0) = \Re\{\mathcal{C}_i(\tau_0, f_0)\} + j\Im\{\mathcal{C}_i(\tau_0, f_0)\}$.

The CAF is crucial in the acquisition (and tracking) of the satellites' signals. For the i-th satellite, the MLE of $\boldsymbol{\theta}$ can be expressed in terms of it as

$$(\hat{\tau}_0, \hat{f}_0) = \arg\max_{\tau_0, f_0} \left\{ |\mathcal{C}_i(\tau_0, f_0)|^2 \right\} \tag{8}$$

$$\hat{\alpha}_0 = \left| \mathcal{C}_i(\hat{\tau}_0, \hat{f}_0) \right| \tag{9}$$

$$\hat{\phi}_0 = \angle \mathcal{C}_i(\hat{\tau}_0, \hat{f}_0) , \tag{10}$$

where $\hat{\alpha}_0$ is the MLE for $\sqrt{2C}$, the LOS signal amplitude. Notice that (10) is in general not used for positioning until noise is filtered out by the phase-tracking loops or when longer integration times can be considered [56]. Such MLE solution is optimal under AWGN assumptions and in the absence of multipath, $y[n] = x[n; \boldsymbol{\theta}] + \eta[n]$. However, it substantially degrades when $M \geq 1$ [4], [7], [57]. The main known effect is that the influence of multipath biases and distorts the CAF that the receiver employs for tracking, ultimately impacting the estimation of LOS' phase, delay, and Doppler variables in $\boldsymbol{\theta}$. This paper presents a data-driven methodology to improve correlation outputs in order to mitigate multipath effects on tracking loops.

III. Data-driven GNSS correlation

The CAF in (6) is optimal under nominal conditions and provides an easy and intuitive way for the receiver to extract the necessary information from the satellites. In this article we aim at augmenting that correlation operation, which has strong foundations rooted on the nominal physical channel, with a data-driven approach that can learn the complexities of the propagation channel. While the proposed data-driven solution could be used in the acquisition stage, it is known that multipath primarily affects tracking loops due to its higher precision and as such we focus on that particular stage of the receiver. This section describes the architecture of the proposed DNN.

A. *Overview of neural network models and notation*

Deep learning involves training a model, that consists of a combination of neurons and layers, by using a large sample of input/output relations referred to as dataset. The neuron is nothing but a parametric function that weights the inputs (through trained weights) and then applies a predefined activation function. A collection of neurons forms a layer. In its basic form, a NN consists of an input layer, an output layer, and an arbitrary number of so-called hidden layers [58].

As shown in Fig. 2, a connection between neuron j in layer $\ell - 1$ and neuron i in layer ℓ is given by the weight w_{ij}^{ℓ}, which represents the significance of the connection between layers, and a bias term b_i is also applied for output y_i^{ℓ} to become [58]:

$$y_i^{\ell} = f_{\ell}(b_i + \sum_{j=1}^{D} w_{ij}^{\ell} y_j^{\ell-1}) \, , \tag{11}$$

where $f_{\ell}(\cdot)$ is the activation function and D is the number of neurons in layer $\ell - 1$. Following (11), the output of layer ℓ is a vector:

$$\mathbf{y}^{\ell} = \mathbf{f}(\mathbf{b}_{\ell} + \mathbf{W}_{\ell}\mathbf{y}^{\ell-1}) = \mathbf{f}_{\ell}(\mathbf{y}^{\ell-1}) \, , \tag{12}$$

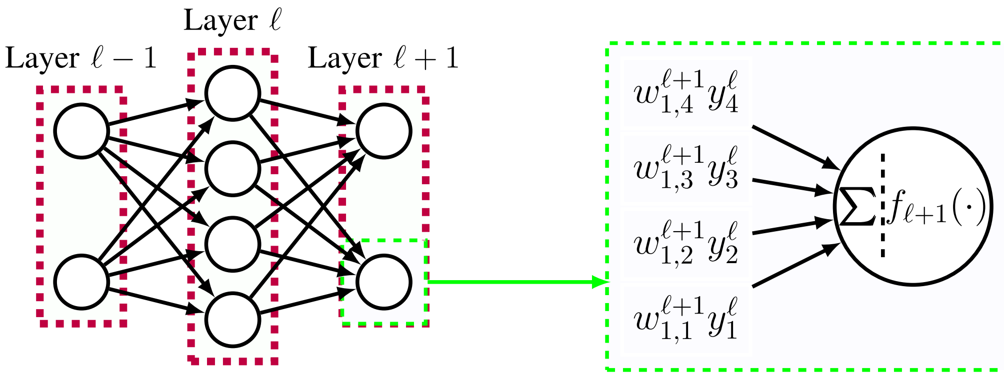

Figure 2: A NN architecture composed of input, hidden, and output layers (left) of neurons (right). In this example, the zoomed neuron has 4 inputs from the previous ℓ-th layer, which are weighted accordingly and added before being nonlinearly transformed through the activation function $f_{\ell+1}(\cdot)$.

where $\mathbf{b}_\ell$ and $\mathbf{W}_\ell$ are vector and matrix forms gathering the biases and weights of the ℓ layer. Thus, the entire NN can be expressed sequentially as a set of nested functions:

$$\mathbf{z} = \mathbf{f}_L \circ \mathbf{f}_{L-1} \circ \cdots \circ \mathbf{f}_1(\mathbf{y}) \tag{13}$$

where L is the total number of layers, $\mathbf{y}$ is the input vector to the NN and $\mathbf{z}$ denotes its final output.

B. Physics-informed, data-driven correlation model

In this article, a DNN is trained specifically to substitute the correlation operation in (6) as typically implemented in tracking loops, shown in the dashed box of Fig. 1. More precisely, the general block diagram of the proposed architecture is shown in Fig. 3, where by comparison to Fig. 1 it can be seen that the NN model is meant to substitute the correlation process, also marked in the dashed box. The input to the DNN is a delayed version of the Pseudo-Random Noise (PRN) code $c_i(nT_s - \tau_0)$ and the GNSS signal after carrier wipe-off. The DNN output is a set of correlation values, where a Prompt and an arbitrary number of Early/Late samples are then fed to the code/phase discriminators for DLL/PLL processing. The initial normalization in Fig. 3 is to scale the amplitude of the signal into the range $[0, 1]$, as is typically done in NNs. The re-scaling at the DNN output aim at incorporating the amplitudes back before correlation outputs are used in the tracking loops.

The main architecture of the proposed DNN for correlation calculation is shown in Fig. 4. In this DNN, the first convolutional layer is fixed with parameters based on the corresponding PRN code $\mathbf{c}_i$ to

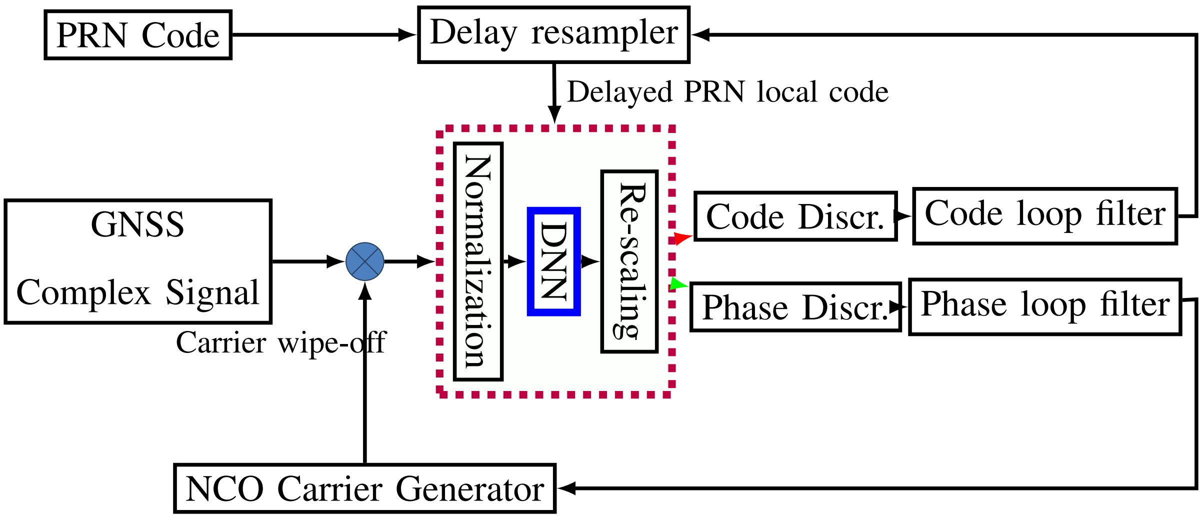

Figure 3: Diagram of the proposed DNN-based correlation scheme, in the dashed box. The goal is to substitute the standard correlation and its usage in tracking loops in order to increase the receiver robustness against multipath.

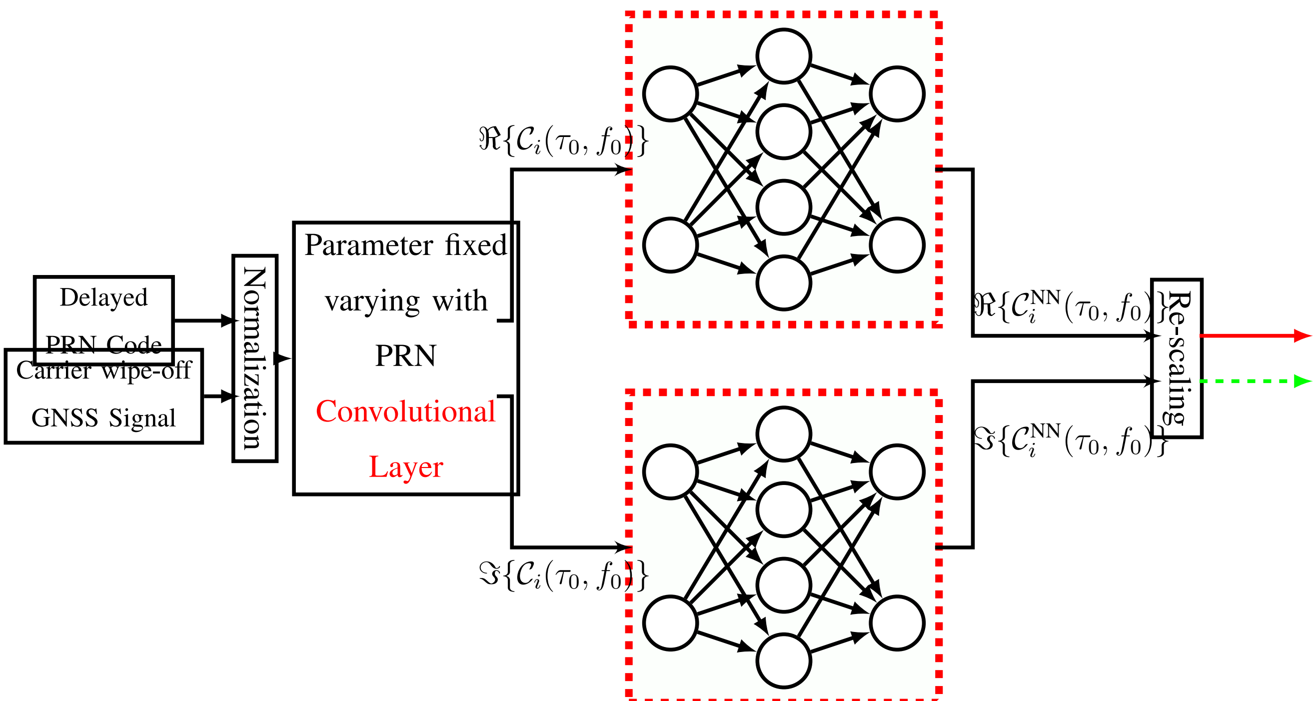

Figure 4: Architecture of the proposed DNN model and its fit within the GNSS receiver architecture. A first convolutional layer encodes the physics-based modeling, while the hidden layers (for both real and imaginary) learns the multipath channel from data.

incorporate the information brought by standard correlation method in (7). The convolutional layer is constructed in a way that is equivalent to the standard correlation process, which can be interpreted as a convolution between the I&Q samples and the local code, thus ensuring that the *physics* of the problem are kept [59]. Then, the real and imaginary parts of standard correlation result (implemented now as a convolution layer of a CNN) are fed to two independent and parallel MLP models for regression. Note that the two regression blocks are the same NNs. The regression output is then the real or imaginary parts of the noiseless correlation result with virtually no multipath effect. Combining the real and imaginary parts, the reconstructed CAF is then

$$\mathcal{C}_i^{\mathrm{NN}}(\tau_0, f_0) = \Re\{\mathcal{C}_i^{\mathrm{NN}}(\tau_0, f_0)\} + j\Im\{\mathcal{C}_i^{\mathrm{NN}}(\tau_0, f_0)\} \tag{14}$$

such that the estimation of the desired LOS signal parameters can be obtained by

$$(\hat{\tau}_0, \hat{f}_0) = \arg\max_{\tau_0, f_0} \left\{ \left|\mathcal{C}_i^{\mathrm{NN}}(\tau_0, f_0)\right|^2 \right\} \tag{15}$$

$$\hat{\alpha}_0 = \left|\mathcal{C}_i^{\mathrm{NN}}(\hat{\tau}_0, \hat{f}_0)\right| \tag{16}$$

$$\hat{\phi}_0 = \angle\mathcal{C}_i^{\mathrm{NN}}(\hat{\tau}_0, \hat{f}_0) \tag{17}$$

in the usual manner.

In practice, the output of the NN can contain an arbitrary number of correlation outputs, among which the necessary Early/Prompt/Late samples can be fed to the tracking loop discriminators. The normalization block before the DNN scales the peak value of correlation results to one, since the satellite signal generated in training stage was set to have unit power. Particularly, such normalization can be computed in practice by a least squares solution whereby the signal amplitude is estimated as

$$\hat{\alpha} = \arg\min_{\alpha} \sum_{n=0}^{N-1} \left| y[n] - \alpha e^{j\phi} c(nT_s - \hat{\tau}_0) e^{j(2\pi \hat{f}_0 n T_s)} \right|^2 \tag{18}$$

which results in $\hat{\alpha} = \left|\mathbf{c}_i^H \mathbf{y}\right|$ with the local code evaluated at $\hat{\tau}_0$ and $\hat{f}_0$ from the previous iteration in the tracking loops. Then the normalization before DNN processing would be such that $\frac{y[n]}{\hat{\alpha}}$ becomes the input DNN signal. Conversely, the normalization is undone at the DNN output as $\hat{\alpha}\mathcal{C}_i^{\mathrm{NN}}(\tau_0, f_0)$

IV. MODEL TRAINING , VALIDATION AND TESTING

In order to test the performance of the model in Fig. 4, a large dataset with representative multipath channel realizations was generated. Multipath channel samples were simulated using the multipath channel model in the ITU-R P.681 recommendation [55], originally developed by the German Aerospace

Center (DLR) [60]. The multipath channel model provides realizations of the Chanel Impulse Response (CIR) according to various receiver dynamics, scenario characteristics, and receiver configurations. A sample power and phase realizations is shown in Fig. 5, where the blue stem represents the LOS channel tap and the red taps correspond to multipath propagation channels for a vehicular urban scenario. Fig. 6 shows an example of $|\mathcal{C}_i(\tau_0, f_0)|^2$ the standard correlation samples $i)$ without multipath (blue); and $ii)$ with the CIR shown in Fig. 5, both under a $C/N_0 = 45$ dB-Hz (C/N_0 denoting the carrier-to-noise-density ratio). It can be observed a clear bias in the correlation peak due to the multipath influence.

For testing purposes, four scenarios were considered depending on the user dynamics (i.e., pedestrian or vehicular) and whether the receiver was in a urban or suburban environment. Namely, pedestrian urban; pedestrian suburban; vehicular urban; and vehicular suburban scenarios. Additionally, a LOS scenario was also generated in the absence of multipath propagation in order to test the performance of the DNN in the nominal case. The DNN was tested using data from all those five scenarios, yielding a model that learned nominal and a variety of propagation channels.

The proposed correlation method was tested in the context of standard tracking loops. For the sake of completeness, different DLL discriminators were considered in order to measure the performance of the proposed NN-based correlation method. When the GNSS signal is perfectly aligned with its local replica, the Prompt correlation result would correspond to $\mathcal{C}_i(\tau_0, f_0)$. In practice, the Prompt sample corresponds to $\mathcal{C}_i(\hat{\tau}_0, \hat{f}_0)$ with $\hat{\tau}_0$ and $\hat{f}_0$ being the most current delay estimates, respectively. Similarly, the Early (and Late) correlation sample would be $\mathcal{C}_i(\hat{\tau}_0 - \frac{d}{2}, \hat{f}_0)$ (for the Late sample, $\mathcal{C}_i(\hat{\tau}_0 + \frac{d}{2}, \hat{f}_0)$) , where d [chips] is typically referred to as the Early-Late (E-L) spacing.

In this article, the conventional Early-minus-Late discriminator is considered, defined as:

$$\mathcal{D}_{E-L}(\hat{\tau}_0) = \frac{|\mathcal{C}_i(\hat{\tau}_0 - \frac{d}{2}, \hat{f}_0)| - |\mathcal{C}_i(\hat{\tau}_0 + \frac{d}{2}, \hat{f}_0)|}{|\mathcal{C}_i(\hat{\tau}_0 - \frac{d}{2}, \hat{f}_0)| + |\mathcal{C}_i(\hat{\tau}_0 + \frac{d}{2}, \hat{f}_0)|} \tag{19}$$

where we considered $d = 1$ chip as the normalized (wide) E-L discriminator and $d = 0.1$ chip as the narrow discriminator. As another point of comparison, the proposed NN based correlation method was used in conjunction of a popular multipath mitigation discriminator known as the High Resolution Correlatior (HRC), or double delta. To keep consistency with the normalized E-L discriminator above, the same normalization factor was considered:

$$\mathcal{D}_{HRC}(\hat{\tau}_0) = \frac{|\mathcal{C}_i(\hat{\tau}_0 - \frac{d}{2}, \hat{f}_0)| - |\mathcal{C}_i(\hat{\tau}_0 + \frac{d}{2}, \hat{f}_0)|}{|\mathcal{C}_i(\hat{\tau}_0 - \frac{d}{2}, \hat{f}_0)| + |\mathcal{C}_i(\hat{\tau}_0 + \frac{d}{2}, \hat{f}_0)|} \tag{20}$$

$$- \frac{1}{2}\frac{(|\mathcal{C}_i(\hat{\tau}_0 - d, \hat{f}_0)| - |\mathcal{C}_i(\hat{\tau}_0 + d, \hat{f}_0)|}{|\mathcal{C}_i(\hat{\tau}_0 - \frac{d}{2}, \hat{f}_0)| + |\mathcal{C}_i(\hat{\tau}_0 + \frac{d}{2}, \hat{f}_0)|} . \tag{21}$$

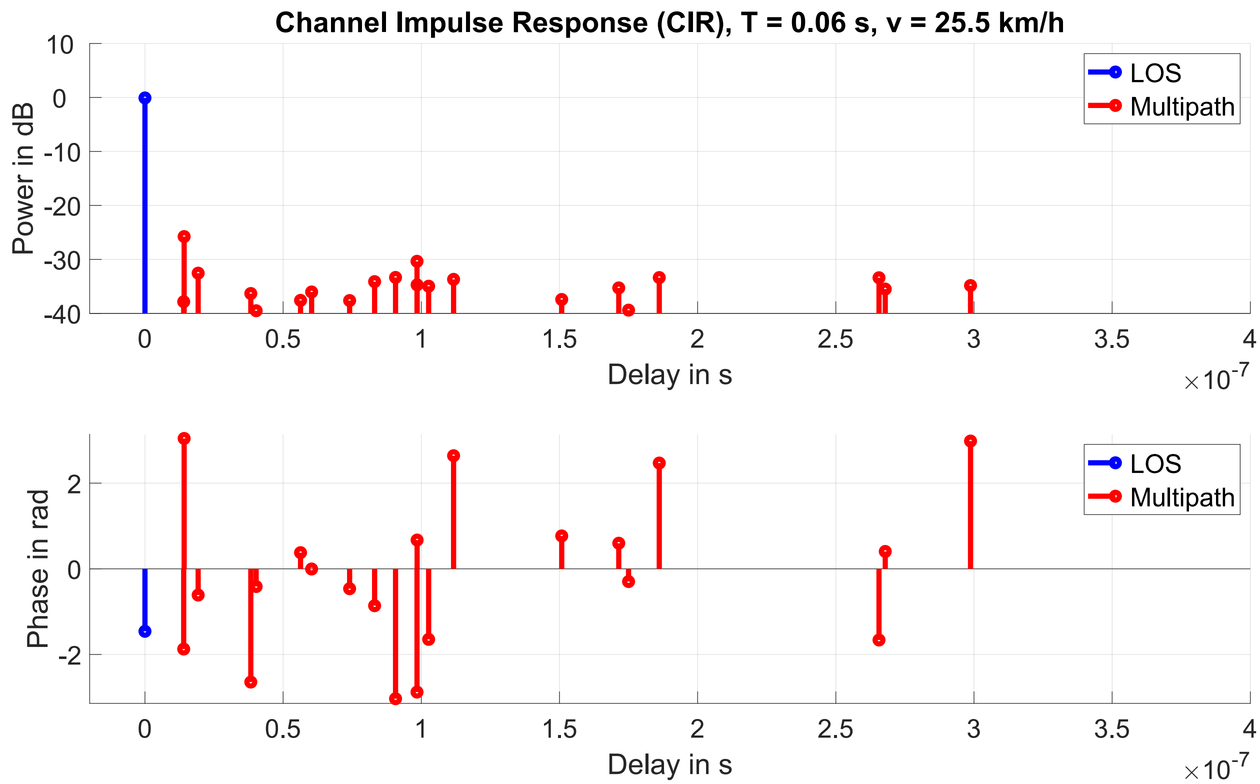

Figure 5: Channel model example in a vehicular urban scenario.

The NN was build as discussed in Section III, with 12 hidden layers and parameters set as detailed in Table. I, with the activation function being leakyReLu, all layers being dense and the selected loss function being the predictive Mean Square Error (MSE). The convolutional layer is in charge of producing $\mathcal{C}_i(\hat{\tau}_0, \hat{f}_0)$, the standard CAF, which is fed to the hidden layers implemented by an MLP to output the enhanced CAF, $\mathcal{C}_i^{\mathrm{NN}}(\hat{\tau}_0, \hat{f}_0)$. In other words, the output of the NN is the real and imaginary parts of the noiseless CAF with virtually no multipath influence, formulated as in (14). The input of the NN (i.e., the regression process) is the corresponding real and imaginary parts of the CAF as produced by the correlators. In particular, the NN was trained with inputs that correspond to the either LOS case (i.e., corrupted with noise only) and multipath-influenced case (i.e., affected by both noise and multipath reflections). More precisely, in the current implementation both CAFs contain 201 correlation samples spaced by 0.025 chips, which is the selected size of both input and output NN layers. The number of layers of the NN was chosen after several trials, observing that fewer layers would degrade

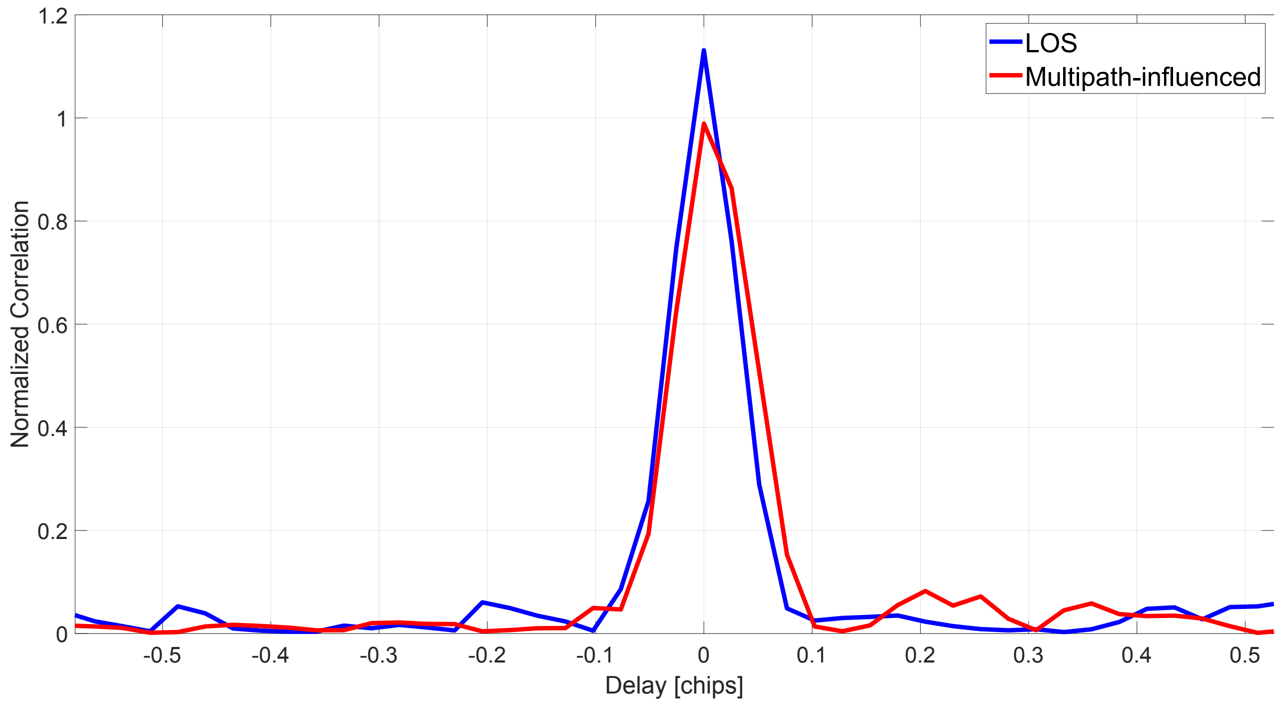

Figure 6: Standard Correlation results under $C/N_0 = 45$ dB-Hz in a vehicular urban scenario. In training, the proposed DNN was fed the LOS correlation as the output. In red, the standard CAF after the multipath channel in Fig. 5.

the performance of the NN-based method in the tracking loop. More automated approaches to select the NN architecture can be considered in future works such as the use of Bayesian Optimization [61], [62]. In the experiments, the NN (hidden layers) is trained and tested with both real and imaginary correlation results. The training dataset was generated under both LOS case (30% of data) and multipath-influenced case (70% of data). In both cases, the satellite signal was simulated with $f_s = 40$ MHz, a random residual Doppler shift in $[-250, 250]$ Hz, a random time-delay error in $[-0.5, 0.5]$ chips, a random carrier phase in $[-0.1\pi, 0.1\pi]$ radians, and a carrier-to-noise-density ratio (CN0) ranging from 35 dB-Hz to 45 dB-Hz. Those random errors are drawn from uniform distributions. Additionally, in multipath-influenced case, a single-ray multipath replica is simulated with a relative time-delay varying from 0 to 2.5 chips and relative amplitude varying from -1 to 1, compared with the true satellite signal. The validating dataset was generated with the same parameter setting. Note that the amount of input-output pairs in both training and validating datasets was $48 \cdot 10^4$. Also, the input vector consisted of the I&Q samples of a

Input	201	2048	2048	1024	1024	512	512	512	512	256	256	128	128
Output	2048	2048	1024	1024	512	512	512	512	256	256	128	128	201
Weights	413696	4196352	2098176	1049600	524800	262656	262656	262656	131328	65792	32896	16512	25856

Table I: Neural network architecture (input/output dimensions and number of weights per layer) of the 11 hidden layers in the architecture shown in Fig. 4.

1 ms integration period, while the output vector produced 201 samples of the NN correlation function $\mathcal{C}_i^{\mathrm{NN}}(\hat{\tau}_0, \hat{f}_0)$. More precisely, real and imaginary components in (14) are produced by two identical hidden layers which transform real and imaginary outputs of the convolutional layer, respectively. The test dataset was generated by the aforementioned channel model from [55], simulating realistic multipath scenarios to assess the performance of the proposed NN in general scenarios.

V. Simulation Analysis

In the experiments, a GPS L5 signal was generated under different scenarios mentioned in Section IV, at a sampling rate of $f_s = 40$ MHz and filtered at 11 MHz. The filtered signal was then processed by the GNSS receiver as usual, first a standard acquisition processing (where the proposed NN-based methodology was not employed) and secondly tracking loops (which use the proposed NN-based method to produce correlation outputs, as well as standard correlation as a benchmark). The result of the acquisition process provided an initialization for the tracking loops, with typical errors on the order of half of a Doppler bin (125 Hz in the experiments [63]) for frequency and half a chip period for delay parameters. The loop bandwidth of the DLL and PLL was set to 2 Hz and 30 Hz, respectively. A $T = 50$ seconds long I&Q signal was generated using the aforementioned ITU realistic channel model [55], which was used to test the trained NN-based correlators.

Fig. 7 presents the filtered DLL discriminator error varying with time as an example to assess the performance of NN-based correlation method in Pedestrian Suburban scenario under different CN0s with three different discriminators. In particular, the figure shows a realization for four different scenarios, showing a comparison between the performance under 35 and 45 dB-Hz CN0 with both 1 ms and 10 ms coherent integration times. In the figure, red lines represent NN-based correlation method and blue lines show performance of standard correlation method as a comparison. In order to focus on the multipath mitigation capabilities of the proposed method, the results neglect the initial convergence period of the tracking loops, which was seen to be similar for both standard and NN-based correlation methods in the experiments run. From Fig. 7, comparing different integration times under both CN0s, we can find that $i)$ the NN-based method has a similar performance as the standard correlation method in terms of their discriminator variances with E-L discriminators; $ii)$ it seems to improve the standard results when considering HRC discriminator; and $iii)$ slightly improves the overall robustness to multipath-induced errors when compared to standard correlation for larger integrations (please see the zoomed areas in the middle, right-most plot of Fig. 7). For shorter integration times, this robustness is more apparent, where it can be observed that the spikes due to multipath biases are attenuated or removed. This can be explained by the longer integration that tends to filter out multipath effects. In such situations, specially when multipath has a limited lifespan, larger integration helps, which might not be the case when either multipath is more persistent (e.g. fixed receiver and scatterer), the dynamics of the receiver are rather slow, or one cannot easily use longer coherent integrations due to the presence of data bits. Given the advantage of NN-based correlation method, a classifier identifying LOS/multipath-influenced cases is no longer needed here (as it was in our earlier works). The high spikes in results of the standard method indicate the occurrence of multipath, while we can clearly see that the NN-based correlation method can reduce those spikes and thus limit multipath influence. The explanation for those results is on the *a priori* knowledge that the DNN gathered from the large training dataset, whereby multipath is learnt and noise is smoothed by a non-linear mapping.

To show more details about NN-based correlation method's performance in different scenarios, Fig. 8 and Fig. 9 show the Cumulative Density Function (CDF) of filtered DLL discriminator error in log scale for $C/N_0 = 35$ dB-Hz and 45 dB-Hz, respectively, both considering 1 ms integration time. The solid lines represent standard correlation results and the dashed lines show performance of NN-based correlation. Three different discriminators were considered in tracking loops in order to understand the performance using different tracking loop schemes. In Fig. 8 and Fig. 9, blue lines represent E-L discriminator, red lines provide performance of narrow discriminator, while the green lines show HRC discriminator performance. The different subplots provide results for different relevant scenarios of the [55] channel model, as well as the no-multipath AWGN case. In the two figures, we can see that when the tracking loops are in lock, NN-based correlation method could generally provide a smaller filtered DLL discriminator error, indicating a much more accurate delay estimation than the standard correlation method, in all four multipath-influenced scenarios as well as the LOS scenario, with all three discriminators.

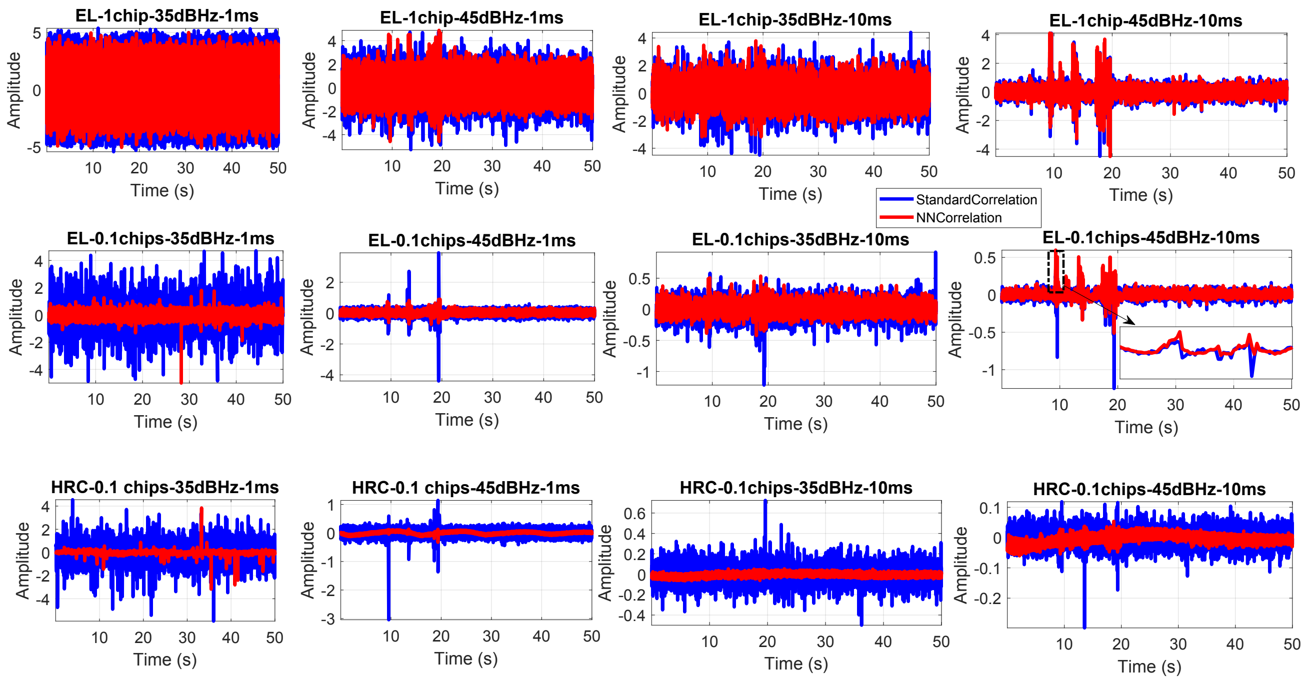

Figure 7: Performance comparison of correlation methods measured by 3 different discriminators (each row) under different CN0s with different coherent integration times in Pedestrian Suburban scenario. Titles of subplots indicate the discriminator type, correlation spacing and considered CN0.

VI. Conclusions

This paper proposes and discusses the use of deep learning as an approach to substitute standard correlation methods in GNSS receivers. The proposed DNN model is, compared to the original work in [54], a simpler (no need to have an additional LOS/multipath-influenced classifier), more versatile (able to learn a variety of propagation conditions), and features a more intuitive reasoning (an upfront convolution layer encapsulates the standard correlation method, while the hidden layers learn the complex channel through data training). Simulations on a tracking loop show that the proposed data-driven approach can not only learn the GNSS correlation operation, but outperform legacy solution in virtually all tested scenarios. It is noted that the investigated NN model requires a multi-correlation scheme, whereby multiple correlation outputs are computed, thus involving an increased computational cost when compared to standard methods. Future work should address complexity reduction and generalization of the model to different receiver configurations, as well as testing on real data.

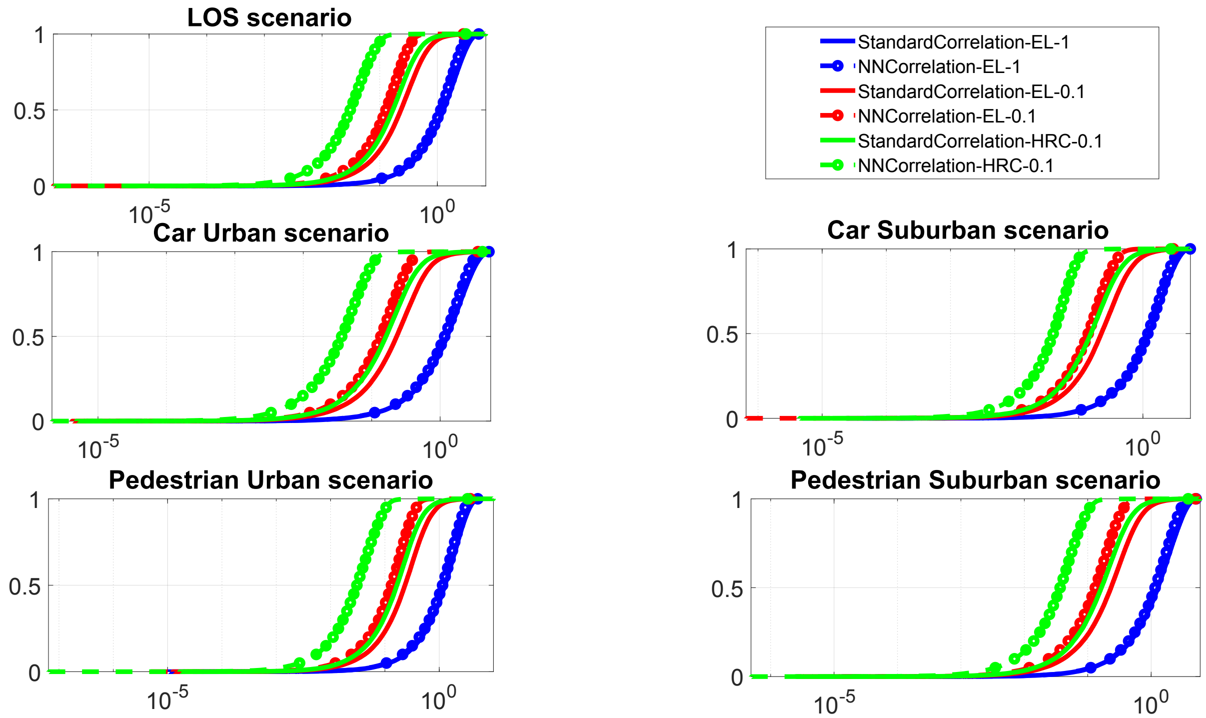

Figure 8: Performance comparison of correlation methods measured by 3 different discriminators in 5 scenarios under $C/N_0 = 35$ dB-Hz.

References

[1] D. Dardari, E. Falletti, and M. Luise, *Satellite and terrestrial radio positioning techniques: a signal processing perspective*. Academic Press, 2011.

[2] M. G. Amin, P. Closas, A. Broumandan, and J. L. Volakis, "Vulnerabilities, threats, and authentication in satellite-based navigation systems [scanning the issue]," *Proceedings of the IEEE*, vol. 104, no. 6, pp. 1169–1173, 2016.

[3] D. Dardari, P. Closas, and P. M. Djurić, "Indoor tracking: Theory, methods, and technologies," *IEEE Transactions on Vehicular Technology*, vol. 64, no. 4, pp. 1263–1278, 2015.

[4] Y. J. Morton, F. van Diggelen, J. J. Spilker Jr, B. W. Parkinson, S. Lo, and G. Gao, *Position, Navigation, and Timing Technologies in the 21st Century: Integrated Satellite Navigation, Sensor Systems, and Civil Applications*. John Wiley & Sons, 2021.

[5] A. Van Dierendonck, P. Fenton, and T. Ford, "Theory and performance of narrow correlator spacing in a GPS receiver," *Navigation*, vol. 39, no. 3, pp. 265–283, 1992.

[6] G. A. McGraw, "GNSS multipath mitigatioin using gated and high resolution correlator concepts," in *Proc. National Technical Meeting of the Satellite Division of the Institute of Navigation, Jan. 1999*, 1999, pp. 333–342.

[7] R. D. Van Nee, J. Siereveld, P. C. Fenton, and B. R. Townsend, "The multipath estimating delay lock loop: approaching theoretical accuracy limits," in *Proceedings of 1994 IEEE Position, Location and Navigation Symposium-PLANS'94*. IEEE, 1994, pp. 246–251.

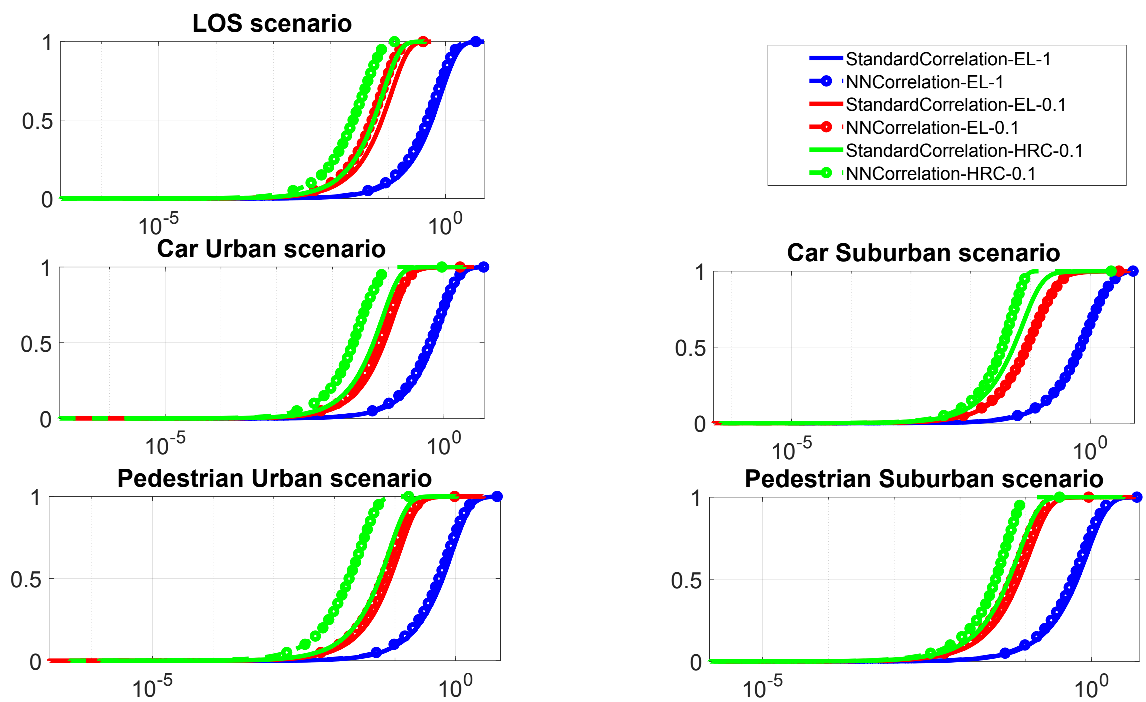

Figure 9: Performance comparison of correlation methods measured by 3 different discriminators in 5 scenarios under $C/N_0 = 45$ dB-Hz.

[8] Z. M. Kassas, P. Closas, and J. Gross, "Navigation systems panel report navigation systems for autonomous and semi-autonomous vehicles: Current trends and future challenges," *IEEE Aerospace and Electronic Systems Magazine*, vol. 34, no. 5, 2019.

[9] D. Medina, K. Gibson, R. Ziebold, and P. Closas, "Determination of pseudorange error models and multipath characterization under signal-degraded scenarios," in *Proceedings of the 31st International Technical Meeting of the Satellite Division of The Institute of Navigation (ION GNSS+ 2018),*. Institute of Navigation, 2018, pp. 3446–3456.

[10] P. Closas, "Bayesian Signal Processing Techniques for GNSS Receivers: From Multipath Mitigation to Positioning," Ph.D. dissertation, 2009.

[11] J. Jones, P. Fenton, B. Smith *et al.*, "Theory and performance of the pulse aperture correlator," in *Proceedings of ION GPS*, vol. 2004, 2004.

[12] A. Van Dierendonck, "Evaluation of GNSS receiver correlation processing techniques for multipath and noise mitigation," in *Proceedings of the National Technical Meeting (ION), 1997*, 1997.

[13] B. Townsend and P. Fenton, "A practical approach to the reduction of pseudorange multipath errors in a L1 GPS receiver," in *Proceedings of the 7th International Technical Meeting of the Satellite Division of the Institute of Navigation, Salt Lake City, UT, USA*. Citeseer, 1994, pp. 20–23.

[14] P. C. Fenton and J. Jones, "The theory and performance of NovAtel Inc.'s vision correlator," in *Proceedings of the ION GNSS*. Citeseer, 2005, pp. 2178–2186.

[15] L. R. Weill, "Multipath mitigation using modernized GPS signals: how good can it get?" in *Proceedings of ION GPS 2002, Portland*

OR, 2002, pp. 493–505.

[16] P. Closas, C. Fernandez-Prades, and J. A. Fernandez-Rubio, "A Bayesian approach to multipath mitigation in GNSS receivers," *IEEE Journal of Selected Topics in Signal Processing*, vol. 3, no. 4, pp. 695–706, 2009.

[17] A. Fernandez, J. Pulido, M. Wis, P. Closas, C. Fernández-Prades, F. Zanier, R. Prieto-Cerdeira, and M. Crisci, "ARTEMISA: Preliminary results of advanced receiver techniques for multipath mitigation," in *Proceedings of the 25th International Technical Meeting of the Satellite Division of The Institute of Navigation (ION GNSS 2012)*, 2012, pp. 1444–1453.

[18] A. Siemuri, H. Kuusniemi, M. S. Elmusrati, P. Välisuo, and A. Shamsuzzoha, "Machine Learning Utilization in GNSS—Use Cases, Challenges and Future Applications," in *2021 International Conference on Localization and GNSS (ICL-GNSS)*. IEEE, 2021, pp. 1–6.

[19] D. Brum, M. R. Veronez, E. M. de Souza, I. É. Koch, L. Gonzaga, I. Klein, M. T. Matsuoka, V. F. Rofatto, A. M. Junior, G. E. dos Reis Racolte *et al.*, "A proposed earthquake warning system based on ionospheric anomalies derived from gnss measurements and artificial neural networks," in *IGARSS 2019-2019 IEEE International Geoscience and Remote Sensing Symposium*. IEEE, 2019, pp. 9295–9298.

[20] M. Alshaye, F. Alawwad, and I. Elshafiey, "Hurricane tracking using Multi-GNSS-R and deep learning," in *2020 3rd International Conference on Computer Applications & Information Security (ICCAIS)*. IEEE, 2020, pp. 1–4.

[21] Q. Yan and W. Huang, "Sea ice sensing from GNSS-R data using convolutional neural networks," *IEEE Geoscience and Remote Sensing Letters*, vol. 15, no. 10, pp. 1510–1514, 2018.

[22] Q. Yuan, H. Shen, T. Li, Z. Li, S. Li, Y. Jiang, H. Xu, W. Tan, Q. Yang, J. Wang *et al.*, "Deep learning in environmental remote sensing: Achievements and challenges," *Remote Sensing of Environment*, vol. 241, p. 111716, 2020.

[23] Y. L. Liu, Y. Morton, and Y. J. Jiao, "Application of Machine Learning to Characterization of GPS L1 Ionospheric Amplitude Scintillation," in *2018 IEEE/ION Position, Location and Navigation Symposium (PLANS)*, 2018, pp. 1159–1166.

[24] N. Linty, A. Farasin, A. Favenza, and F. Dovis, "Detection of GNSS ionospheric scintillations based on machine learning decision tree," *IEEE Transactions on Aerospace and Electronic Systems*, vol. 55, no. 1, pp. 303–317, 2018.

[25] L. Mallika, D. V. Ratnam, S. Raman, G. Sivavaraprasad *et al.*, "Machine learning algorithm to forecast ionospheric time delays using global navigation satellite system observations," *Acta Astronautica*, vol. 173, pp. 221–231, 2020.

[26] R. O. Perez, "Using TensorFlow-based Neural Network to estimate GNSS single frequency ionospheric delay (IONONet)," *Advances in Space Research*, vol. 63, no. 5, pp. 1607–1618, 2019.

[27] K. Lamb, G. Malhotra, A. Vlontzos, E. Wagstaff, A. G. Baydin, A. Bhiwandiwalla, Y. Gal, A. Kalaitzis, A. Reina, and A. Bhatt, "Prediction of GNSS phase scintillations: A machine learning approach," *arXiv preprint arXiv:1910.01570*, 2019.

[28] M. O. Selbesoglu, "Prediction of tropospheric wet delay by an artificial neural network model based on meteorological and GNSS data," *Engineering Science and Technology, an International Journal*, vol. 23, no. 5, pp. 967–972, 2020.

[29] J. Vilà-Valls, N. Linty, P. Closas, F. Dovis, and J. T. Curran, "Survey on signal processing for GNSS under ionospheric scintillation: Detection, monitoring, and mitigation," *NAVIGATION, Journal of the Institute of Navigation*, vol. 67, no. 3, pp. 511–536, 2020.

[30] M. R. Manesh, J. Kenney, W. C. Hu, V. K. Devabhaktuni, and N. Kaabouch, "Detection of GPS spoofing attacks on unmanned aerial systems," in *2019 16th IEEE Annual Consumer Communications & Networking Conference (CCNC)*. IEEE, 2019, pp. 1–6.

[31] P. Borhani-Darian, H. Li, P. Wu, and P. Closas, "Deep Neural Network Approach to Detect GNSS Spoofing Attacks," in *Proceedings of the 33rd International Technical Meeting of the Satellite Division of The Institute of Navigation (ION GNSS+ 2020)*, 2020, pp. 3241–3252.

[32] S. Tohidi and M. R. Mosavi, "Effective detection of GNSS spoofing attack Using A multi-layer perceptron neural network classifier trained by PSO," in *2020 25th International Computer Conference, Computer Society of Iran (CSICC)*. IEEE, 2020, pp. 1–5.

[33] R. Calvo-Palomino, A. Bhattacharya, G. Bovet, and D. Giustiniano, "Short: Lstm-based gnss spoofing detection using low-cost spec-

trum sensors," in *2020 IEEE 21st International Symposium on" A World of Wireless, Mobile and Multimedia Networks"(WoWMoM)*. IEEE, 2020, pp. 273–276.

[34] S. Semanjski, A. Muls, I. Semanjski, and W. De Wilde, "Use and validation of supervised machine learning approach for detection of GNSS signal spoofing," in *2019 International Conference on Localization and GNSS (ICL-GNSS)*. IEEE, 2019, pp. 1–6.

[35] R. Morales Ferre, A. de la Fuente, and E. S. Lohan, "Jammer classification in GNSS bands via machine learning algorithms," *Sensors*, vol. 19, no. 22, p. 4841, 2019.

[36] A. Louis and M. Raimondi, "Neural network based evil waveforms detection," in *Proceedings of the 33rd International Technical Meeting of the Satellite Division of The Institute of Navigation (ION GNSS+ 2020)*, 2020, pp. 1984–1989.

[37] M. Mosavi and F. Shafiee, "Narrowband interference suppression for GPS navigation using neural networks," *GPS solutions*, vol. 20, no. 3, pp. 341–351, 2016.

[38] Z. Zhang, F. Wu, Y. Liu, Y. Zuo, and Y. Ji, "A neural network aided integrated navigation algorithm based on vehicle motion mode information," in *2019 IEEE International Conference on Signal Processing, Communications and Computing (ICSPCC)*. IEEE, 2019, pp. 1–5.

[39] H.-f. Dai, H.-w. Bian, R.-y. Wang, and H. Ma, "An INS/GNSS integrated navigation in GNSS denied environment using recurrent neural network," *Defence technology*, vol. 16, no. 2, pp. 334–340, 2020.

[40] Z. Zou, T. Huang, L. Ye, and K. Song, "CNN based adaptive kalman filter in high-dynamic condition for low-cost navigation system on highspeed UAV," in *2020 5th Asia-Pacific Conference on Intelligent Robot Systems (ACIRS)*. IEEE, 2020, pp. 103–108.

[41] Y. Quan, L. Lau, G. W. Roberts, X. Meng, and C. Zhang, "Convolutional neural network based multipath detection method for static and kinematic GPS high precision positioning," *Remote Sensing*, vol. 10, no. 12, p. 2052, 2018.

[42] R. Sun, L.-T. Hsu, D. Xue, G. Zhang, and W. Y. Ochieng, "GPS signal reception classification using adaptive neuro-fuzzy inference system," *The Journal of Navigation*, vol. 72, no. 3, pp. 685–701, 2019.

[43] L.-T. Hsu, "GNSS multipath detection using a machine learning approach," in *2017 IEEE 20th International Conference on Intelligent Transportation Systems (ITSC)*. IEEE, 2017, pp. 1–6.

[44] B. Guermah, H. EL Ghazi, T. Sadiki, and H. Guermah, "A robust GNSS LOS/multipath signal classifier based on the fusion of information and machine learning for intelligent transportation systems," in *2018 IEEE International Conference on Technology Management, Operations and Decisions (ICTMOD)*. IEEE, 2018, pp. 94–100.

[45] G. Zhang, P. Xu, H. Xu, and L.-T. Hsu, "Prediction on the Urban GNSS Measurement Uncertainty Based on Deep Learning Networks With Long Short-Term Memory," *IEEE Sensors Journal*, vol. 21, no. 18, pp. 20 563–20 577, 2021.

[46] N. I. Ziedan, "Optimized Position Estimation in Multipath Environments using Machine Learning," in *Proceedings of the 34th International Technical Meeting of the Satellite Division of The Institute of Navigation (ION GNSS+ 2021)*, 2021, pp. 3437–3451.

[47] G. Caparra, P. Zoccarato, and F. Melman, "Machine Learning Correction for Improved PVT Accuracy," in *Proceedings of the 34th International Technical Meeting of the Satellite Division of The Institute of Navigation (ION GNSS+ 2021)*, 2021, pp. 3392–3401.

[48] P. Borhani-Darian and P. Closas, "Deep Neural Network Approach to GNSS Signal Acquisition," in *2020 IEEE/ION Position, Location and Navigation Symposium (PLANS)*. IEEE, 2020, pp. 1214–1223.

[49] M. Orabi, J. Khalife, A. A. Abdallah, Z. M. Kassas, and S. S. Saab, "A machine learning approach for GPS code phase estimation in multipath environments," in *2020 IEEE/ION Position, Location and Navigation Symposium (PLANS)*. IEEE, 2020, pp. 1224–1229.

[50] C. Savas and F. Dovis, "Multipath Detection based on K-means Clustering," in *Proceedings of the 32nd International Technical Meeting of the Satellite Division of The Institute of Navigation (ION GNSS+ 2019)*, 2019, pp. 3801–3811.

[51] T. Suzuki, K. Kusama, and Y. Amano, "NLOS Multipath Detection using Convolutional Neural Network," in *Proceedings of the 33rd International Technical Meeting of the Satellite Division of the Institute of Navigation (ION GNSS+ 2020)*, 2020, pp. 2989–3000.

[52] Q. Liu, Z. Huang, and J. Wang, "Indoor non-line-of-sight and multipath detection using deep learning approach," *GPS Solutions*, vol. 23, no. 3, pp. 1–14, 2019.

[53] E. Munin, A. Blais, and N. Couellan, "Convolutional neural network for multipath detection in GNSS receivers," in *2020 International Conference on Artificial Intelligence and Data Analytics for Air Transportation (AIDA-AT)*. IEEE, 2020, pp. 1–10.

[54] H. Li, P. Borhani-Darian, P. Wu, and P. Closas, "Deep learning of GNSS signal correlation," in *Proceedings of the 33rd International Technical Meeting of the Satellite Division of The Institute of Navigation (ION GNSS+ 2020)*, 2020, pp. 2836–2847.

[55] ITU-R P.2145-2, "Model Parameters for the Physical-Statistical Wideband Model in Recommendation ITU-R P.681," Sep. 2017.

[56] X. Liu, M. Á. Ribot, A. Gusi-Amigó, A. Rovira-Garcia, J. S. Subirana, and P. Closas, "Cloud-Based Single-Frequency Snapshot RTK Positioning," *Sensors*, vol. 21, no. 11, p. 3688, 2021.

[57] K. Borre, D. M. Akos, N. Bertelsen, P. Rinder, and S. H. Jensen, *A software-defined GPS and Galileo receiver: a single-frequency approach*. Springer Science & Business Media, 2007.

[58] C. M. Bishop, *Pattern recognition and machine learning*. springer, 2006.

[59] T. Imbiriba, A. Demirkaya, J. Duník, O. Straka, D. Erdoğmuş, and P. Closas, "Hybrid neural network augmented physics-based models for nonlinear filtering," in *FUSION conference*, Linkoping, Sweden, 4-7 July 2022.

[60] A. Lehner and A. Steingass, "Software model for satellite to land mobile multipath propagation ." 2019. [Online]. Available: https://www.KNS.dlr.de/COSLMS

[61] T. Yu and H. Zhu, "Hyper-parameter optimization: A review of algorithms and applications," *arXiv preprint arXiv:2003.05689*, 2020.

[62] C. White, W. Neiswanger, and Y. Savani, "BANANAS: Bayesian Optimization with Neural Architectures for Neural Architecture Search," in *Proceedings of the AAAI Conference on Artificial Intelligence*, 2021.

[63] C. Fernández–Prades, J. Arribas, P. Closas, C. Avilés, and L. Esteve, "GNSS-SDR: An open source tool for researchers and developers," in *Proc. 24th Intl. Tech. Meeting Sat. Div. Inst. Navig.*, Portland, Oregon, Sept. 2011, pp. 780–794.

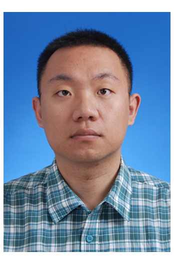

Haoqing Li received the BS degree in electrical engineering from Wuhan University, China, in 2016 and the MS degree in electrical and computer engineering from Northeastern University, Boston, MA, in 2018, where he is currently working toward the Ph.D. degree in electrical and computer engineering. His research interests include GNSS signal processing, anti-jamming technology, deep learning and robust statistics.

Parisa Borhani-Darian received her BS and MS degrees in Computer Engineering at Qazvin University in Iran. She is currently a PhD candidate in the Department of Electrical and Computer Engineering at Northeastern University, Boston, MA. Her current research is on Deep Neural Networks for GNSS signal acquisition and spoofing detection for safety in connected vehicles.

Peng Wu received his BS degree in Physics from Tianjin University of Technology, China in 2012 and MS degree in Electrical Engineering from Northeastern University, Boston, MA, in 2018. He is currently a PhD candidate in the Department of Electrical and Computer Engineering at Northeastern University. His research interests include distributed data fusion and machine learning with applications to indoor positioning and tracking.

Pau Closas (Senior Member, IEEE), is an Associate Professor in Electrical and Computer Engineering at Northeastern University, Boston MA. He received the MS and PhD in Electrical Engineering from UPC in 2003 and 2009, respectively. He also holds a MS in Advanced Maths and Mathematical Engineering from UPC since 2014. He is the recipient of the EURASIP Best PhD Thesis Award 2014, the 9^{th} Duran Farell Award for Technology Research, the 2016 ION's Early Achievements Award, 2019 NSF CAREER Award, and the IEEE AESS Harry Rowe Mimno Award in 2022. His primary areas of interest include statistical signal processing, stochastic filtering, robust filtering, and machine learning, with applications to positioning and localization systems. He volunteered in editorial roles (e.g. NAVIGATION, Proc. IEEE, IEEE Trans. Veh. Tech., and IEEE Sig. Process. Mag.), and has been actively involved in organizing committees of a number of conference such as EUSIPCO (2011, 2019-2022), IEEE SSP'16, IEEE/ION PLANS (2020, 2023), or IEEE ICASSP'20.